ANTIOXIDANTS & REDOX SIGNALING
Volume 20, Number 4, 2014

DOI: 10.1089/ars.2013.5236

ORIGINAL RESEARCH COMMUNICATION

Glutathione Peroxidase 7 Utilizes Hydrogen Peroxide Generated by Ero1α to Promote Oxidative Protein Folding

Lei Wang,[1] Lihui Zhang,[1,2] Yingbo Niu,[1,2] Roberto Sitia,[3] and Chih-chen Wang[1]

Abstract

Aims: Ero1 flavoproteins catalyze oxidative folding in the endoplasmic reticulum (ER), consuming oxygen and generating hydrogen peroxide (H_2O_2). The ER-localized glutathione peroxidase 7 (GPx7) shows protein disulfide isomerase (PDI)-dependent peroxidase activity *in vitro*. Our work aims at identifying the physiological role of GPx7 in the Ero1α/PDI oxidative folding pathway and at dissecting the reaction mechanisms of GPx7. ***Results:*** Our data show that GPx7 can utilize Ero1α-produced H_2O_2 to accelerate oxidative folding of substrates both *in vitro* and *in vivo*. H_2O_2 oxidizes Cys57 of GPx7 to sulfenic acid, which can be resolved by Cys86 to form an intramolecular disulfide bond. Both the disulfide form and sulfenic acid form of GPx7 can oxidize PDI for catalyzing oxidative folding. GPx7 prefers to interact with the *a* domain of PDI, and intramolecular cooperation between the two redox-active sites of PDI increases the activity of the Ero1α/GPx7/PDI triad. ***Innovation:*** Our *in vitro* and *in vivo* evidence provides mechanistic insights into how cells consume potentially harmful H_2O_2 while optimizing oxidative protein folding *via* the Ero1α/GPx7/PDI triad. Cys57 can promote PDI oxidation in two ways, and Cys86 emerges as a novel noncanonical resolving cysteine. ***Conclusion***: GPx7 promotes oxidative protein folding, directly utilizing Ero1α-generated H_2O_2 in the early secretory compartment. Thus, the Ero1α/GPx7/PDI triad generates two disulfide bonds and two H_2O molecules at the expense of a single O_2 molecule. *Antioxid. Redox Signal.* 20, 545–556.

Introduction

Oxidative folding is vital for the structure and function of most secretory and membrane proteins. In the endoplasmic reticulum (ER), disulfide bond formation is catalyzed by members of the protein disulfide isomerase (PDI) family, which typically possess CXXC active sites that are used in interchange reactions (12). Ero1 flavoproteins re-oxidize PDI and enable continuous transfer of disulfides to substrate proteins (2, 26). They do so using O_2 as an electron acceptor and producing equimolar hydrogen peroxide (H_2O_2) for each disulfide formed (11, 34). Particularly in professional secretory cells, this pathway could cause oxidative stress. How do cells deal with excess H_2O_2 in the ER? First, yeast and mammalian Ero1 proteins are elegantly regulated by feedback mechanisms, which limit reactive oxygen species production through futile cycling (1, 3, 13, 27, 35). Second, H_2O_2 could introduce disulfides into folding substrates (17, 20), either directly or through specialized enzymes. Among the latter, peroxiredoxin 4 (Prx4) can catalyze *de novo* disulfide formation at the expense of H_2O_2 (28, 39). However, Prx4 can be

Innovation

To catalyze oxidative folding, Ero1-flavoproteins yield hydrogen peroxide (H_2O_2) in stoichiometric amounts to the disulfides formed. We show that glutathione peroxidase 7 (GPx7) can utilize Ero1α-produced H_2O_2 *in vitro* and *in vivo* to oxidize protein disulfide isomerase (PDI) and accelerate oxidative folding. The peroxidase activity of GPx7 reveals novel mechanistic features of the catalytic and resolving cysteines. The Ero1α/GPx7/PDI triad couples H_2O_2 elimination and disulfide generation to ensure efficient and safe oxidative protein folding.

[1]National Laboratory of Biomacromolecules, Institute of Biophysics, Chinese Academy of Sciences, Beijing, China.
[2]University of Chinese Academy of Sciences, Beijing, China.
[3]Division of Genetics and Cell Biology, Università Vita-Salute San Raffaele Scientific Institute, Milan, Italy.

over-oxidized and inactivated by H_2O_2 (36), and *Prx4* knockout mice have only a minor phenotype (14), implying the existence of other H_2O_2 scavengers in the secretory compartment. Recently, two ER-located glutathione peroxidases (GPx7 and GPx8) were reported to catalyze protein refolding in the presence of PDI and H_2O_2 *in vitro*, with GPx7 being more efficient (22). Loss of GPx7 resulted in systemic oxidative stress damage, increased carcinogenesis, and shortened life span in mice (37). However, the cell-biological evidence for the role of GPx7/8 in disulfide formation is still lacking. So far, the effect of activities of Prx4 and GPx7/8 on oxidative folding was analyzed using exogenous or artificially generated H_2O_2 (22, 39). We investigated whether GPx7 can use Ero1-produced H_2O_2 *in situ* for catalyzing disulfide formation. In this article, we focused on GPx7 for its higher *in vitro* activity compared with GPx8 (22).

GPx7 lacks the loop which determines glutathione (GSH) specificity and oxidizes PDI more efficiently than GSH, implying that GPx7 belongs to the family of thioredoxin GPx-like peroxidases (TGPx) (22, 29). In GPx7, the first cysteine residue Cys57 was supposed to be the peroxidatic cysteine (C_P), as it is located in the -NVASxC(U)G- reactive (seleno)cysteine-containing motif. The second cysteine residue Cys86 is located in the -FPCNQF- motif that is highly conserved among all GPx homologues, but its function remains to be clarified. Intriguingly, a canonical resolving cysteine (C_R) in a 'Cys block' region, essential for completing the catalytic cycle of reduction by thioredoxin in typical two-cysteine TGPx, is missing in GPx7 (7, 29). Therefore, GPx7 was defined as an unusual cysteine-based TGPx, and the reaction mechanisms for GPx7 peroxidase activity were, hence, the other main aim of this study.

Our mutagenesis experiments show that Cys57 of GPx7 is oxidized by H_2O_2 to sulfenic acid, while Cys86 acts as a noncanonical $C_{R,}$ resolving the sulfenylated Cys57 into an intramolecular disulfide bond. Both the disulfide and sulfenic acid forms of GPx7 can oxidize PDI. We demonstrate, moreover, that GPx7 can utilize Ero1α-produced H_2O_2 to accelerate oxidative folding not only *in vitro* but also *in vivo*. In this way, GPx7 allows cells to exploit the potentially harmful peroxides produced by Ero1 to improve oxidative folding, with water being released rather than any reactive oxygen species. Thus, the Ero1α/GPx7/PDI triad represents an efficient and safe oxidative folding system.

Results

GPx7 accelerates oxidative protein folding in Ero1α/PDI system in vitro

We previously reported that human Ero1 proteins consume one molecule of O_2 to produce one disulfide in reduced thioredoxin and equimolar H_2O_2 (34, 35). Here, we show that GPx7 harbors TGPx activity and can use Ero1α-derived H_2O_2 to promote the oxidation of thioredoxin. In this system, one O_2 was consumed to produce two disulfides in thioredoxin with no H_2O_2 detected (Supplementary Fig. S1; Supplementary Data are available online at www.liebertpub.com/ars). Then, we used a physiological substrate, RNase A, instead of the artificial substrate thioredoxin to further dissect the processes of oxidative folding. On addition of exogenous H_2O_2, GPx7 very efficiently co-operated with PDI to catalyze RNase A re-oxidation (Fig. 1A). Next, we examined whether GPx7 could directly use Ero1α-generated H_2O_2 in RNase A re-oxidation by monitoring oxygen consumption. Oxidation of 40 μM denatured and reduced RNase A (containing 160 μM disulfides) by Ero1α and PDI generated $\sim$16 μM H_2O_2 (Fig. 1B), suggesting that some of the peroxides produced were used to generate disulfides directly or with the assistance of PDI in the re-oxidation of multiple disulfides-containing substrates (17). On GPx7 addition, the time needed for the completion of oxygen consumption was, at least, 10 min shorter, and H_2O_2 was no longer detected at the end of the reaction (Fig. 1B). Finally, 86 μM O_2 was consumed, corresponding to two disulfides formed per molecule of O_2. Importantly, in the presence of both Ero1α and PDI, GPx7 was also able to promote RNase A reactivation (Fig. 1C), increasing the rate of RNase A re-oxidation by $\sim$50% (Fig. 1D). When the reduced/oxidized glutathione (GSH/GSSG) redox buffer was used to supply oxidizing power with no H_2O_2 generated, GPx7 did not exert any effect and was not itself oxidized (Supplementary Fig. S2). Bovine GPx1, an enzyme that can quench H_2O_2 but cannot be reduced by PDI (22), did not promote but slightly retarded the reactivation of RNase A (Fig. 1C). Similarly, the addition of GPx7 to a mixture of Ero1α, PDI, and GSH resulted in accelerated GSSG production as well as increased oxygen consumption rate (Supplementary Fig. S3). The results cited earlier demonstrated that GPx7 can facilitate oxidative folding *in vitro* using H_2O_2 generated by Ero1α.

GPx7 is an efficient H_2O_2 scavenger

Of the three tryptophan residues in GPx7, Trp142 is conserved in the GPx family and located close to the C_P active site protein data bank code (PDB: 2P31). On H_2O_2 addition, a time-dependent decrease of intrinsic GPx7 fluorescence was observed, mainly corresponding to quenching of Trp142 fluorescence by H_2O_2-oxidized active site. The fluorescence was then increased markedly, probably due to local conformation changes on prolonged H_2O_2 treatment (Fig. 2A). In the presence of a large excess of H_2O_2 for kinetics study, the rapid initial decrease in fluorescence was fitted to a single exponential function, representing a pseudo-first-order reaction (see *inset* in Fig. 2A). The rate constant for this reaction was linearly increasing in a range of 0.5–10 mM H_2O_2 (Fig. 2B), with the second-order rate constant of $2.6\times10^3\,M^{-1}\cdot s^{-1}$ calculated, which is comparable to that of a synuclein-fused mouse GPx7 ($9.5\times10^3\,M^{-1}\cdot s^{-1}$) (6), and is about 30- and 300-fold greater than that for the reaction of H_2O_2 with GPx8 and PDI (22), respectively. These kinetic data indicate that GPx7 is a very efficient H_2O_2 scavenger.

Cys57 is the C_P and Cys86 is a noncanonical C_R in GPx7

Mature GPx7 contains two cysteines, Cys57 and Cys86. To identify their roles, we replaced either one (GPx7 C57A and GPx7 C86A) or both (GPx7 DM) with alanine and examined their redox states by using 4-acetamido-4′-maleimidylstilbene-2,2′-disulfonic acid (AMS), which reacts with cysteine thiols and adds 500 Da for each modification (Fig. 3A). In the experimental conditions utilized, AMS did not affect the mobility of GPx7 DM, confirming its specific binding to cysteine residues; the single cysteine mutants migrated comparatively slower, indicating that both Cys57 and Cys86 can be modified. Accordingly, GPx7 wild-type (WT) migrated even slower than the single cysteine mutants. After treatment with H_2O_2, GPx7 C57A still displayed the retarded mobility shift

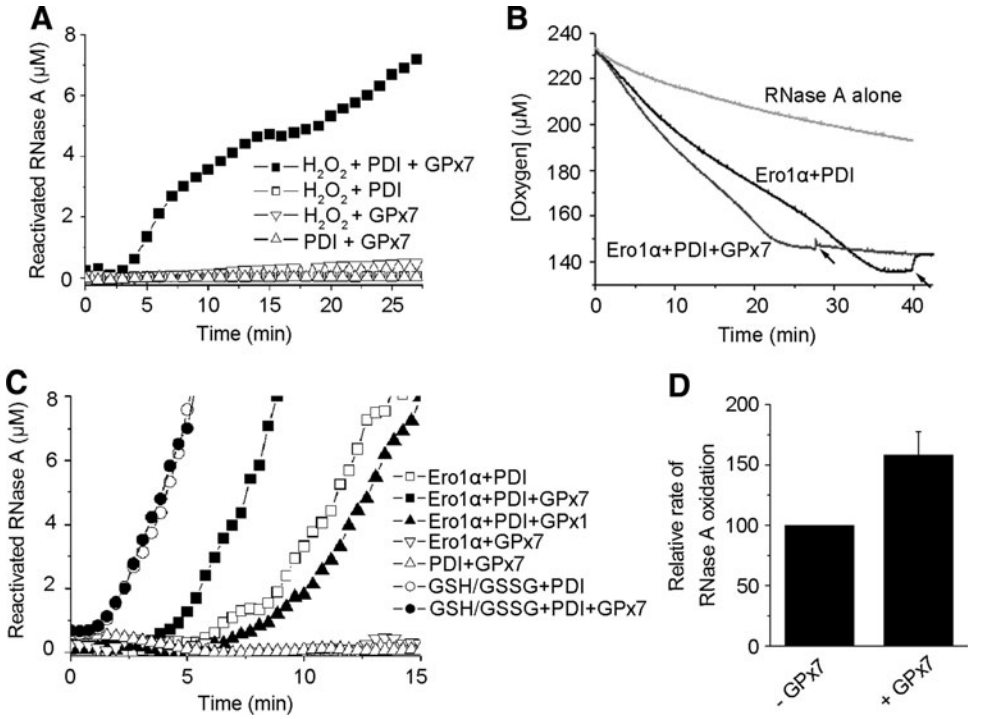

FIG. 1. Glutathione peroxidase 7 (GPx7) synergizes with Ero1 and protein disulfide isomerase (PDI) to accelerate oxidative folding *in vitro*. (A) RNase A (8 μM) reactivation was followed by monitoring the hydrolysis of 4.5 m*M* cCMP in the presence of hydrogen peroxide (H_2O_2) (50 μM), PDI (3 μM), and/or GPx7 (10 μM) as indicated. **(B)** Oxygen consumption was monitored as denatured, and reduced RNase A (40 μM) was re-oxidized alone or in the presence of 3 μM Ero1α and 10 μM PDI, with or without 10 μM GPx7. Catalase was added at the indicated time points (*arrows*). One out of two independent experiments with similar profiles is shown here. **(C)** RNase A (8 μM) reactivation was monitored in the presence of PDI (3 μM), Ero1α (3 μM), GPx7 (10 μM), GPx1 (1 unit), and/or reduced/oxidized glutathione (GSH/GSSG) redox buffer (1/0.2 m*M*) as indicated. **(D)** The relative rate of RNase A oxidation was calculated by measuring the reciprocal of the lag time before the appearance of active RNase A ($n = 3$), as described (34).

while C86A lost AMS reactivity, indicating that Cys57 but not Cys86 reacts with H_2O_2. Strikingly, H_2O_2-treated GPx7 WT migrated even faster than the C86A and DM mutants (compare *lane 9* with *11 and 12*), which is a characteristic of long-range intramolecular disulfide formation. The redox states of GPx7 and its mutants were further confirmed by methoxy polyethylene glycol maleimide alkylation assays, which also resulted in gel-shift retardation (Supplementary Fig. S4).

Next, we used the sulfenic acid-specific reagent, dimedone-based probe 3-(2,4-dioxocyclohexyl) propyl with a biotin tag (DCP-Bio1) (18), to characterize the reaction products of GPx7 and H_2O_2. Consistent with the notion that Cys57 can be sulfenylated by H_2O_2 and acts as the C_P, GPx7 C86A but not C57A was detected by horseradish peroxidise-labeled streptavidin after treating with H_2O_2 and DCP-Bio1 (Fig. 3B). GPx7 WT was not modified, suggesting fast formation of an intramolecular disulfide between the sulfenylated Cys57 and Cys86, which is consistent with the pronounced mobility shift observed in Figure 3A. Thus, Cys86 plays the resolving function but is a noncanonical C_R.

Both the disulfide form and sulfenic acid form of GPx7 are active to oxidize PDI

GPx7 is an efficient PDI peroxidase with extremely weak activity toward GSH (22). To investigate the underlying

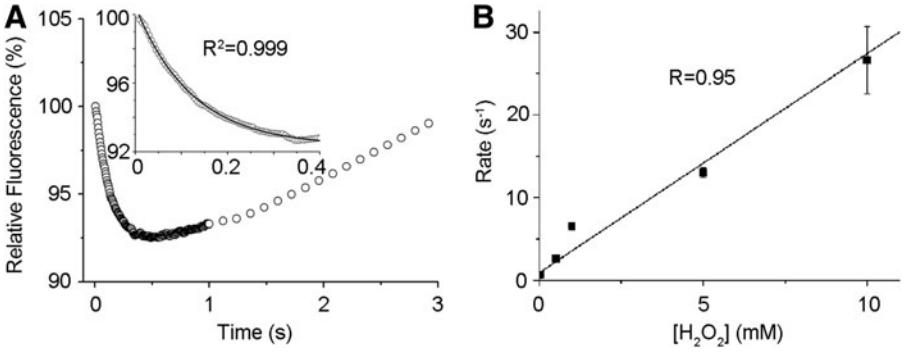

FIG. 2. Kinetics of GPx7 oxidation by H_2O_2. (A) Stopped-flow trace of time-dependent changes in the intrinsic fluorescence of 10 μM GPx7 on addition of 1 m*M* H_2O_2. The initial reaction fits well to a pseudo-first-order reaction (*inset*). **(B)** Linear dependence of the pseudo-first-order rate constant for GPx7 oxidation on the concentration of H_2O_2 ($n \geq 3$).

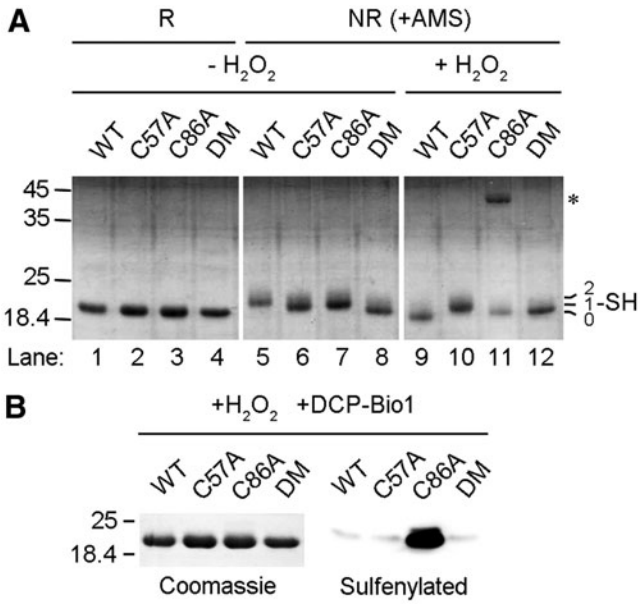

FIG. 3. Cys57 is sulfenylated by H_2O_2 and resolved by Cys86 to form an intramolecular disulfide. (A) The indicated GPx7 variants were incubated without (*lanes 1–8*) or with H_2O_2 (*lanes 9–12*), treated with (*lanes 5–12*) or without (*lanes 1–4*) the alkylating agent 4-acetamido-4′-maleimidylstilbene-2,2′-disulfonic acid (AMS), and resolved by nonreducing (NR, *lanes 5–12*) or reducing (R, *lanes 1–4*) sodium dodecyl sulfate-15% polyacrylamide gel electrophoresis (SDS-15% PAGE). Asterisk indicates GPx7 homodimers formed on H_2O_2 treatment. The numbers of thiols modified by AMS were indicated on the right margin. One representative experiment out of three is shown. **(B)** The indicated GPx7 variants were incubated with H_2O_2 and a biotin-tagged probe (DCP-bio1) specific to sulfenic acid, resolved by SDS-15% PAGE, and analyzed by Coomassie staining (*left panel*) to monitor the loaded sample and by Western blots (WB) (*right panel*) to detect the sulfenylated GPx7.

reaction mechanisms, we determined the enzymatic activities of GPx7 mutants. GPx7 C86A was as active as WT; in contrast, both C57A and DM were inactive (Fig. 4A). C86A also accelerated RNase A refolding when H_2O_2 was generated by Ero1α, while C57A or DM showed little, if any, effect (Fig. 4B). Thus, Cys57 of GPx7 is critical for PDI peroxidase activity. AMS modification assays were then used to determine changes in the redox state of GPx7 and PDI during the reaction. A single PDI active domain was used instead of full-length PDI in these experiments, because the redox shift is more evident in molecules of lower molecular weight. As shown in Figure 4C, the reduced PDI *a* domain was gradually oxidized after equimolar H_2O_2 addition, and was completed after 30 min. Conversely, the intramolecular disulfide form of GPx7 WT due to immediate oxidation by H_2O_2 gradually shifted to the reduced form. GPx7 C86A with the sulfenylated C_P also oxidized PDI *a* domain, albeit less efficiently than WT, which is probably due to the formation of less-active C86A homodimers in the absence of reducing equivalents in the system. Neither mutant lacking C_P (C57A or DM) oxidized PDI *a* domain. Next, to identify the PDI-reacting cysteine in GPx7, we examined complex formation between GPx7 and PDI in the absence of H_2O_2. A mutant PDI (C56A) was used, because replacing the C-terminal cysteine in the CGHC active site allows trapping mixed disulfides in interchange reactions (15). PDI C56A formed covalent complexes of ~70 kDa only with GPx7 C86A (Fig. 4D), indicating that Cys57 forms mixed disulfides with PDI which are resolved by Cys86. Taken together, the results cited earlier suggest that both the disulfide form and sulfenic acid form of GPx7 can directly oxidize PDI and accelerate disulfide formation in substrates, although with different kinetics.

GPx7 accelerates oxidation of reduced J chain in cells depending on Ero1α activity

To investigate whether GPx7 can promote oxidative protein folding in living cells, we monitored disulfide bond formation in myc-tagged Ig J chains (JcM) (21). When HeLa transfectants expressing the reporter were briefly exposed to dithiothreitol (DTT), most JcM migrated as reduced monomers with a few homodimers (Fig. 5A, *lane 1*). On removal of the reducing agent, oxidized species (monomers, dimers, and high-molecular-weight complexes) progressively appeared (*lane 4*). As previously described (21), in cells co-expressing Ero1α, oxidized JcM monomers were detected already at the end of the pulse (*lane 5*), and dimers and high-molecular-weight species formed more rapidly during the chase, confirming that Ero1α functions as an efficient sulfhydryl oxidase. Co-expression of GPx7 resulted in accelerated disappearance of reduced JcM monomers, albeit to a lesser extent compared with Ero1α (compare, for instance, *lanes 9 and 5*, or *11 and 7*). Densitometric quantifications confirmed that GPx7 promotes the oxidation of reduced JcM in living cells (Fig. 5B). Intriguingly, on GPx7 overexpression, fewer JcM-containing covalent complexes accumulated and could be detected only on prolonged exposure (Supplementary Fig. S5). These JcM-containing covalent complexes could still be detected immediately after DTT treatment when Ero1α was overexpressed (Fig. 5A, *lane 5*), which may represent the "old" molecules that are trapped in partially DTT-resistant complexes in this non-radioactive chase (5). It might be also possible that these covalent complexes were the consequence of indiscriminate oxidation by H_2O_2, which resulted from robust Ero1α oxidase activity after DTT challenge, and they were inhibited by the peroxidase activity of GPx7.

Even if expressed at comparable levels, the cysteine mutants GPx7 C57A and DM were less efficient than WT in inducing the disappearance of reduced JcM monomers (Fig. 5C). GPx7 C86A retained partial activity (Fig. 5D). These observations confirm that Cys57 plays a critical role for peroxidase activity also *in vivo*, and the presence of Cys86 as a C_R is important for catalyzing disulfide formation in cells.

To provide further evidence that the effect of GPx7 on oxidative folding is dependent on Ero1α activity, endogenous Ero1α was knocked down by expressing Ero1α-targeting short hairpin RNA (shEro1α). Reduced JcM monomers in control cells disappeared faster at 30°C than at 20°C (compare *lanes 1–4* in Fig. 5E, A). On Ero1α knockdown, the re-oxidation of JcM was significantly delayed (Fig. 5E, *lanes 5–8*), in line with the observation that the restoration of ER redox homeostasis after DTT challenge is compromised by Ero1α depletion (31). Ectopic expression of GPx7 on the background of Ero1α knockdown did not have a significant effect on JcM re-oxidation (Fig. 5F), strongly suggesting that the acceleration effect of GPx7 on JcM re-oxidation was dependent on Ero1α

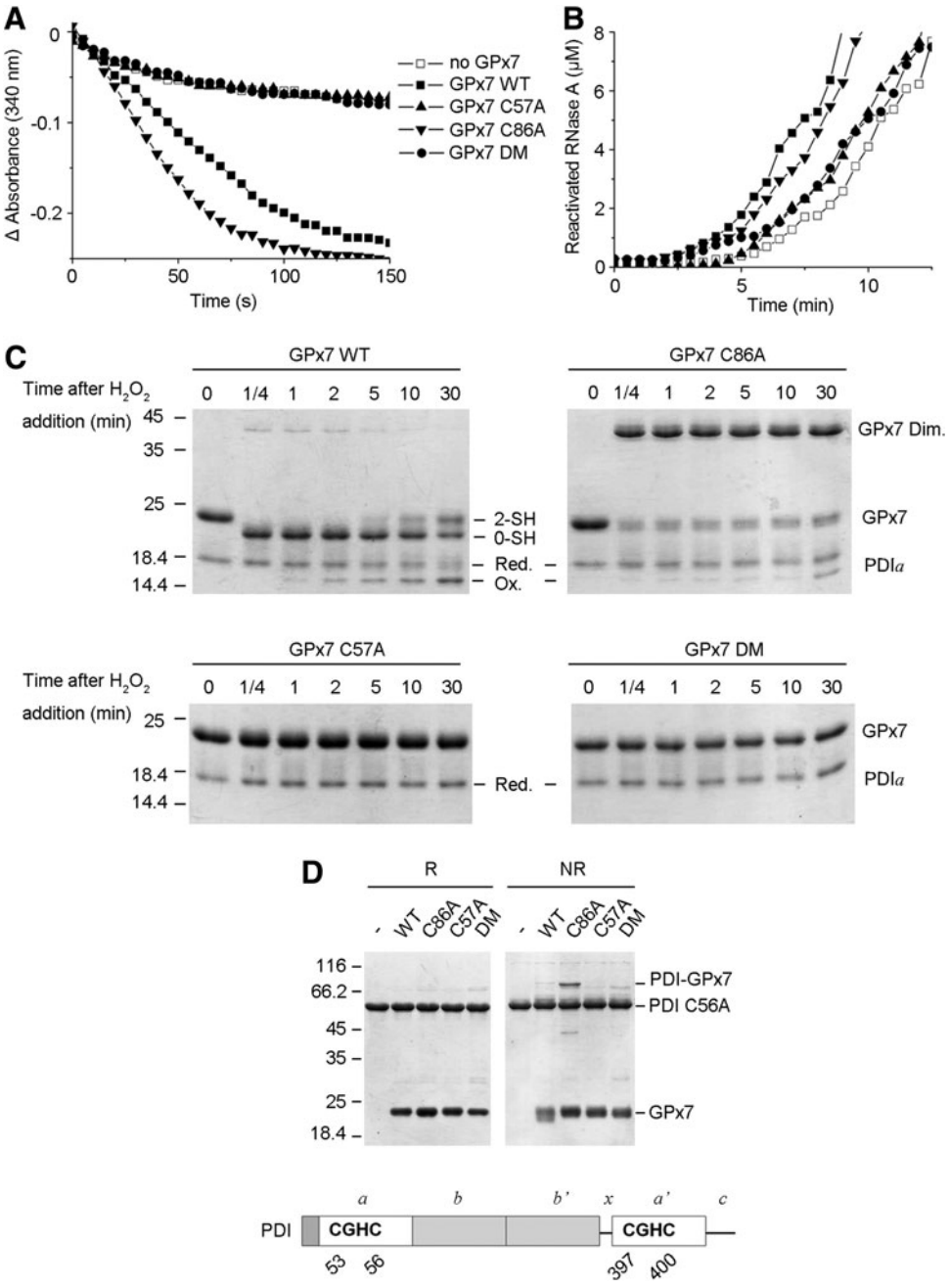

FIG. 4. Cys57 of GPx7 is required for PDI peroxidase activity. (A) GPx activity was measured after the decrease in absorbance at 340 nm due to reduced nicotinamide adenine dinucleotide phosphate (NADPH) consumption by glutathione reductase, in the presence of 40 μM H_2O_2, 0.5 mM GSH, and 10 μM PDI, with or without 10 μM GPx7 mutants. **(B)** RNase A (8 μM) reactivation was determined in the presence of 3 μM Ero1α and PDI with or without the indicated GPx7 mutants (10 μM). **(C)** The change in the redox status of PDI *a* domain after incubation with the indicated GPx7 variants and H_2O_2 was analyzed by nonreducing SDS-15% PAGE after alkylation with AMS. The reduced (Red.) and oxidized (Ox.) forms of PDI *a* domain are indicated. The reduced (2-SH) and intramolecular disulfide form (0-SH) in GPx7 wild type (WT) are indicated as well. One representative experiment out of two is shown. **(D)** GPx7 variants were incubated with PDI C56A, blocked by N-ethylmaleimide (NEM), and then resolved by reducing (R) or non-reducing (NR) SDS-12% PAGE. The domain architecture and CGHC active sites of PDI are schematically illustrated in the *lower panel*.

activity. The results cited earlier implied that in living cells, GPx7 can efficiently utilize Ero1α-derived H_2O_2, which should be the main source of H_2O_2 produced after reductive challenge.

GPx7 and Ero1α bind to PDI separately

Having determined that GPx7 potentiates the Ero1α/PDI system *in vitro* and *in vivo*, we performed glutathione S-transferase (GST)-pulldown studies to detect possible binary or ternary complexes. Approximately 4% of PDI from HeLa cell lysates specifically bound to GST-GPx7 WT or DM chimeras. Ero1α was not detected in the bound fraction (Fig. 6A). Thus, PDI can bind to GPx7 through noncovalent interactions.

We once again took advantage of the PDI cysteine trapping mutants to analyze the ability of the *a* and *a′* domains to covalently interact with GPx7 in HeLa cells. Clearly, as shown in Figure 6B, the covalent GPx7-PDI complexes were more abundant with PDI C56A (* in *lanes 2 and 11*) than with PDI C400A (** in *lanes 3 and 12*), and these bands faded on DTT treatment. After removal of the reducing agent, the complex between GPx7 and PDI *a* domain re-emerged at 30 min (*lanes 8 and 17*). These mixed disulfides likely reflect intermediates in the oxidation of PDI by H_2O_2 catalyzed by GPx7 in cells. Altogether, these results indicate that GPx7 interacts preferentially with the PDI *a* domain.

Interactions between Ero1α, GPx7, and PDI were further investigated by overexpressing Ero1α, GPx7 C86A, and PDI C56A in combinations (Fig. 6C). Ero1α covalently bound to

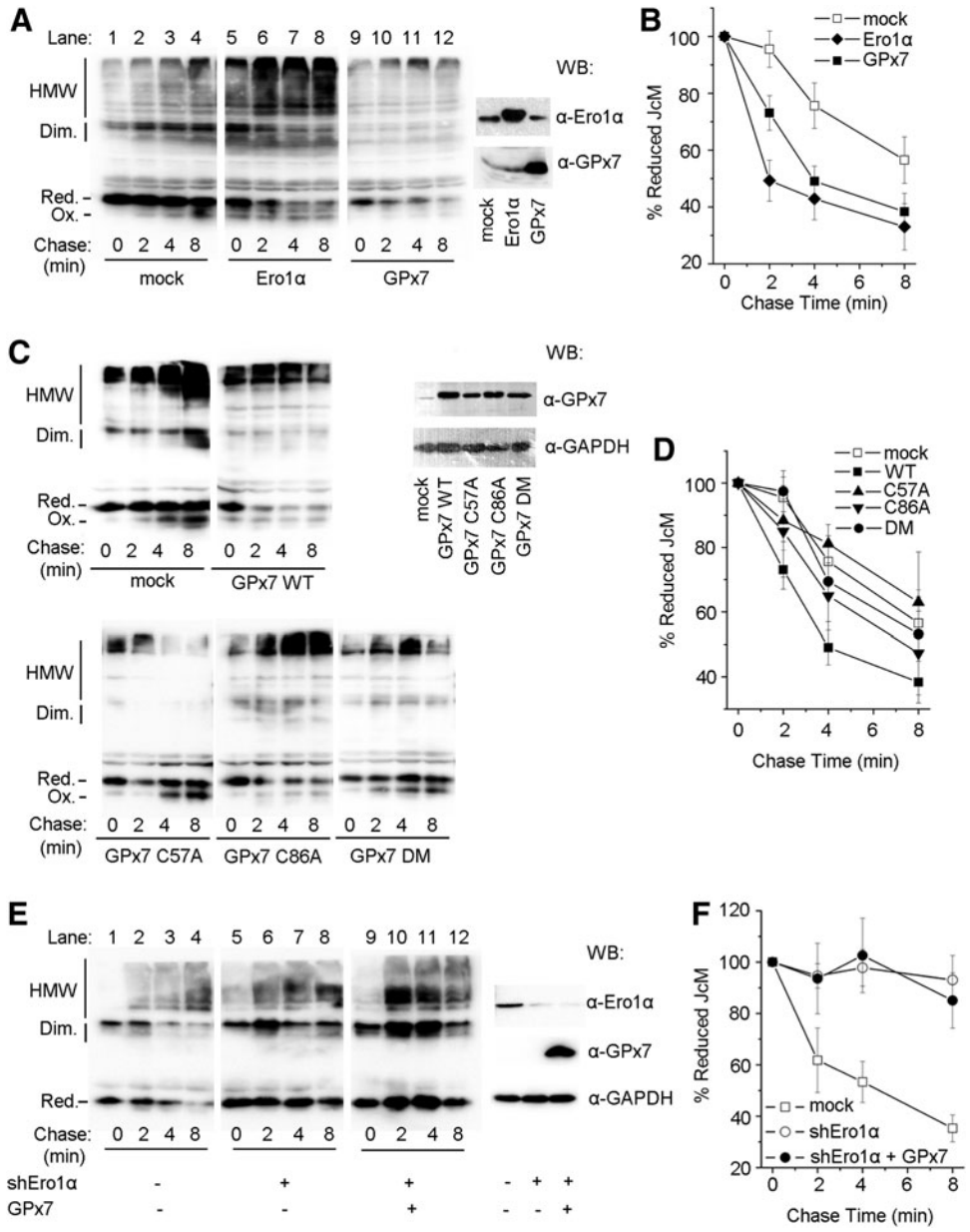

FIG. 5. GPx7 accelerates oxidative protein folding *in vivo*. HeLa transfectants expressing JcM alone (mock), or combined with Ero1α, GPx7 **(A),** or its cysteine mutants **(C)** were treated with dithiothreitol (DTT), washed, and incubated without reducing agent at 20°C for the indicated time. After NEM blocking, cell lysates were analyzed by nonreducing SDS-PAGE and decorated by anti-myc. The mobility of reduced JcM monomers (Red.), oxidized monomers (Ox.), homodimers, and high-molecular-weight complexes (HMW) is indicated. Each sample at 0 min was resolved by reducing SDS-12% PAGE and decorated with anti-Ero1α or anti-GPx7 antibodies. **(E)** JcM expressing HeLa cells were co-transfected with or without shEro1α and GPx7 plasmid as indicated. Experiments were carried out as in **(A)**, except that the incubation after DTT washout was at 30°C, at which JcM oxidation in mock cells was faster than at 20°C, and the effects of Ero1α knockdown were more distinct. The disappearance of fully reduced JcM monomers in **(A)**, **(C),** and **(E)** was quantified by densitometry and plotted as the percent remaining at each time point relative to 0 min in **(B)**, **(D),** and **(F)**, respectively ($n \geq 3$, mean ± S.D.).

endogenous PDI (see bands indicated by open *arrowheads* in *lanes 4 and 9*), likely *via* the *a*′ domain (25), and to both *a* and *a*′ domains in PDI C56A mutant (see bands indicated by open and closed *arrowheads* in *lanes 3 and 8*). GPx7 C86A was linked to the *a* domain of PDI C56A (see bands indicated by diagonal *arrows* in *lanes 2 and 12*, and also see Fig. 6B). When the three proteins were co-expressed together in cells, the binary complexes (PDI-Ero1α and PDI-GPx7) were clearly visible. In contrast, bands corresponding to ternary complex were not detected (compare, for instance, *lanes 10 and 8*, or *15 and 12*), suggesting that GPx7 and Ero1α covalently bind to PDI in a sequential way rather than simultaneously.

Two active sites of PDI cooperate intramolecularly in the Ero1α/GPx7/PDI system

In order to dissect the Ero1α/GPx7/PDI system in greater detail, we measured the amount of the disulfides generated by monitoring GSH oxidation into GSSG *in vitro*. Consistent with the notion that PDI metabolizes H_2O_2 inefficiently (22), very few disulfides were formed in the presence of exogenous H_2O_2 only (Fig. 7A, *white*). The presence of GPx7 markedly accelerated disulfide bond formation catalyzed by PDI WT. In the presence of GPx7, PDIC1 and PDIC2 mutants, in which both cysteines were replaced by serines in the *a* and *a*′ domain active sites separately, catalyzed GSH oxidation by H_2O_2, albeit less efficiently than PDI WT. Mixing PDIC1 and PDIC2 restored the peroxidase activity for GPx7, similar with PDI WT (Fig. 7A, *black*). Thus, GPx7 can readily oxidize either active site of PDI with excess H_2O_2.

Next, Ero1α was used to supply an oxidizing source instead of exogenous H_2O_2. In accordance with a previous finding that Ero1α preferentially oxidizes the *a*′ active site in PDI (3, 34), PDIC1 was able to generate disulfides. In contrast, a few disulfides were produced by PDIC2 (Fig. 7B, *white*). As expected, GPx7 was active toward PDIC1 but inactive toward

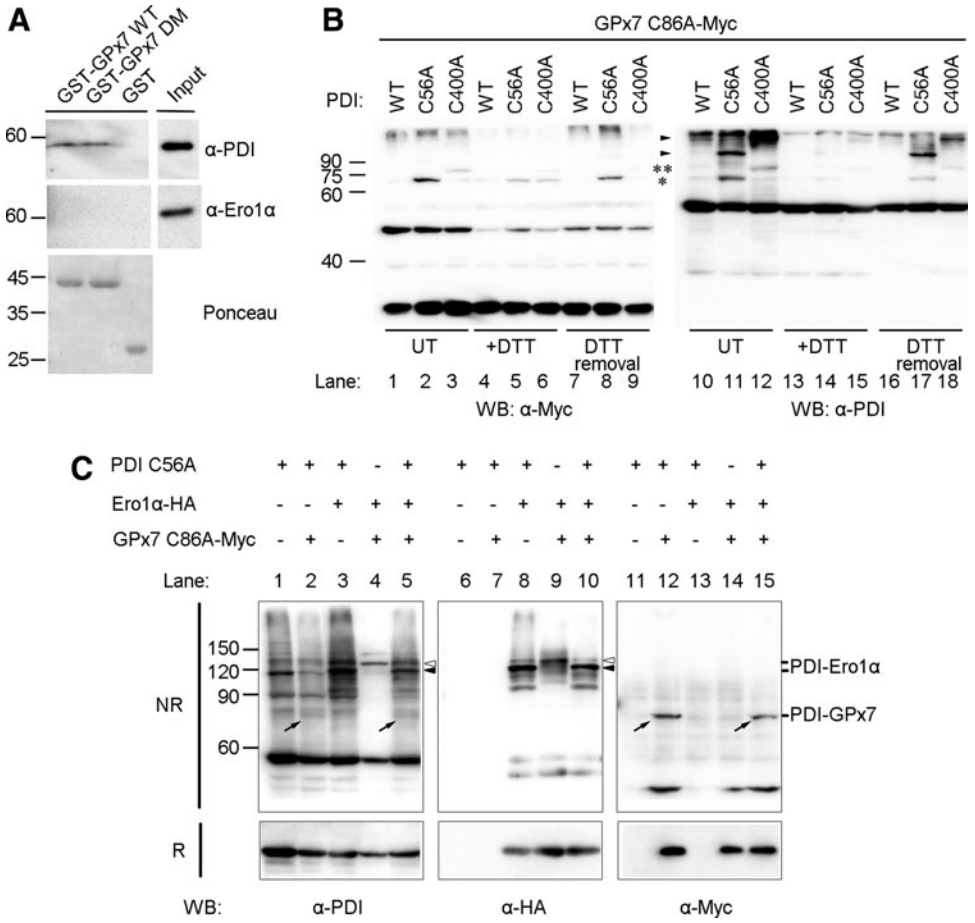

FIG. 6. Formation of covalent binary complexes by GPx7, Ero1α, and PDI. (A) Aliquots of glutathione S-transferase (GST)-GPx7 WT, GST-GPx7 DM, or GST were incubated with HeLa cell lysates and precipitated with GSH-Sepharose. The precipitated proteins and 1/10 of the whole lysates (Input) were analyzed by WB with anti-PDI or anti-Ero1α. PDI, but not Ero1α, was detected in the precipitated fractions. Ponceau staining (*lower panel*) was used to visualize GST-chimeric proteins. **(B)** PDI WT or the two CGHA trapping mutants (C56A and C400A) were co-expressed in HeLa cells with myc-tagged GPx7 C86A. Aliquots of untreated (UT) cells or those treated with exogenous reducing agent (+DTT) were modified with NEM, resolved by SDS-12% PAGE under nonreducing conditions, and decorated with anti-myc or anti-PDI. After DTT treatment, some cells were washed and cultured for 30 min in DTT-free medium (DTT removal) to follow the formation of intermolecular complexes. The single (*) or double asterisks (**) point at adducts between Cys57 of GPx7 and the N-terminal cysteines of *a* or *a*′ PDI active sites, respectively. The *arrowheads* indicated the disulfide-linked complexes between PDI and other client proteins (*e.g.*, Ero1s). **(C)** PDI C56A, HA-tagged Ero1α, and myc-tagged GPx7 C86A were expressed in combinations in HeLa cells. Cells were treated by NEM, and lysates were resolved under nonreducing (NR, 8% SDS-PAGE) or reducing (R, 12%) conditions and decorated with antibodies as indicated. The open and closed *arrowheads* point to the mixed disulfides formed between Ero1α and PDI *a*′ and *a* domains, respectively. The diagonal *arrows* indicate the complexes between GPx7 and PDI. Notice that the exposure time for the *left panel* is shorter than that for the *right panel* and **(B)** in order to make the abundant PDI-Ero1α complexes not too strong to be distinguished; although the bands corresponding to PDI-GPx7 complexes are somehow faint, they are clearly seen in the *right panel* and **(B)**.

PDIC2, as Ero1α does not oxidize the *a* active site producing little H_2O_2. Nevertheless, the activity of GPx7 toward PDIC1 was lower than toward PDI WT, suggesting that the active *a* domains contribute to the interactions with GPx7, although not involved in binding Ero1α. However, adding PDIC2 (with intact *a* domain) to PDIC1 did not increase the activity in the Ero1α/GPx7/PDI system (Fig. 7B, *black*), which is different from using exogenous H_2O_2 as the oxidizing source. The fact that PDIC1 and PDIC2 did not show any synergy for GPx7 in this system suggested that the H_2O_2 produced on the oxidation of PDI *a*′ domain by Ero1α can only be efficiently used by GPx7 to oxidize the *a* domain of the same PDI molecule. Thus, maximal activity of the Ero1α/GPx7/PDI triad requires intramolecular co-operation between the *a* and *a*′ sites in PDI.

Discussion

We have reconstructed an efficient, ER-based oxidative folding system composed of a sulfhydryl oxidase (Ero1α), an oxidoreductase/isomerase (PDI), and a peroxidase (GPx7). Our *in vitro* and *in vivo* assays enable the depiction of a working model for the Ero1α/GPx7/PDI triad (Fig. 8A). Ero1α preferentially oxidizes the *a*′ domain of PDI, generating one molecule of H_2O_2 and a partially oxidized PDI at the

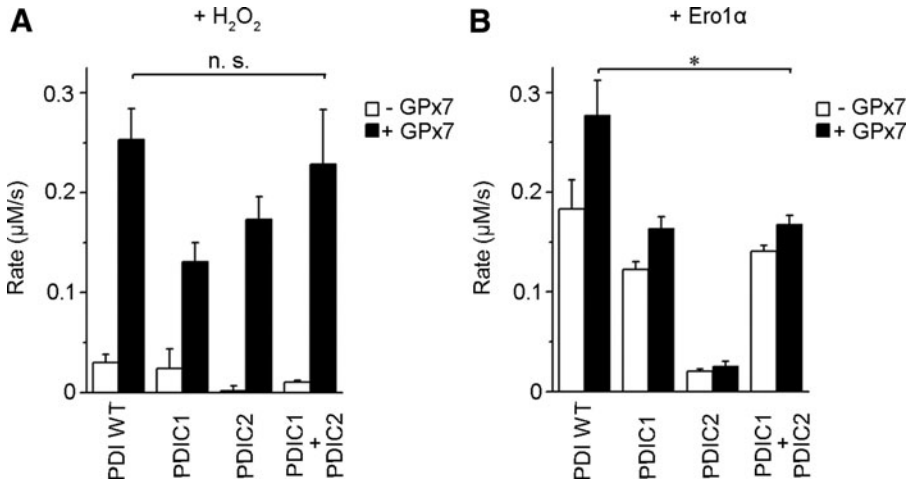

FIG. 7. Intramolecular cooperation between the two PDI active sites. (A) GPx activity was measured on NADPH oxidation in the presence of glutathione reductase with 0.5 m*M* GSH and 0.2 m*M* H_2O_2 as described (22), in the presence of 10 μM PDI or its active site mutants PDIC1 (SGHS in the *a* domain) and PDIC2 (SGHS in the *a*′ domain), with or without 10 μM GPx7, as indicated. **(B)** GPx activity was measured with 2 μM Ero1α to generate H_2O_2, in the presence of 10 μM PDI and 5 m*M* GSH, as sufficient GSH is required for reduction of the regulatory disulfides during Ero1α activation (unpublished data). The rates of NADPH consumption were calculated, which correspond to the rates of disulfide formation ($n \geq 3$, mean ± S.D.). Asterisk indicates statistical significance ($p < 0.05$); n.s., not significant.

expense of one O_2 molecule (Step I). GPx7 uses the H_2O_2 generated by Ero1α *in situ* for oxidizing the *a* domain of the same PDI molecule, preventing diffusion of this reactive oxygen species (Step II). Fully oxidized PDI transfers disulfides into substrates for oxidative folding. *Via* this mechanism, a single O_2 molecule can generate two disulfide bonds and two harmless H_2O molecules. A bimolecular fluorescence complementation experiment in cells suggested a possible physical association between Ero1α and GPx7 (22), and our model suggests that Ero1α and GPx7 preferentially bind to the *a*′ and *a* domain of PDI separately in a sequential way, and maybe transiently close to each other. There are other potential

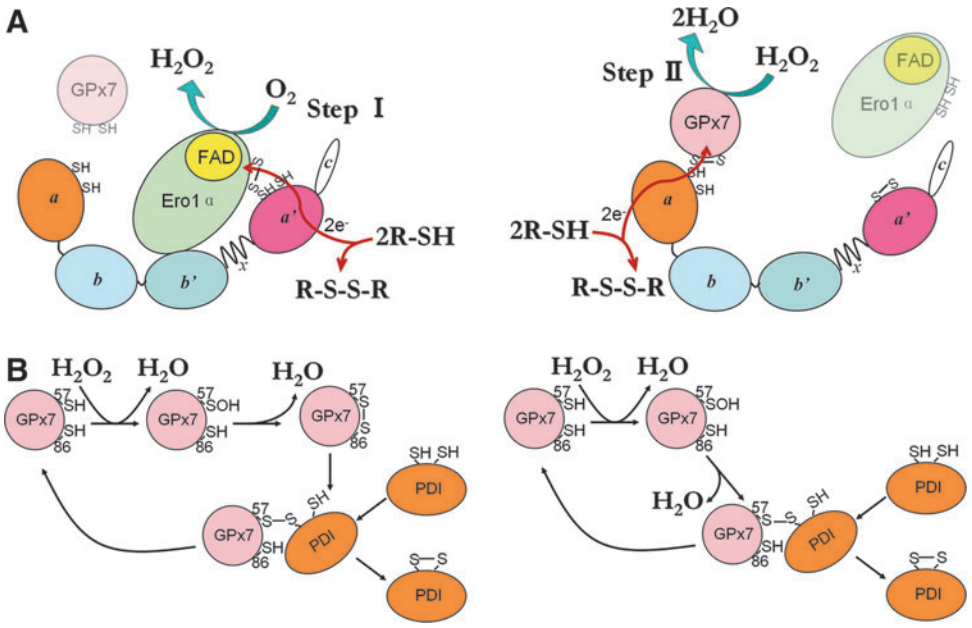

FIG. 8. Schematic model of the Ero1α/GPx7/PDI triad in oxidative protein folding. (A) The *a*′ domain of PDI is oxidized by Ero1α, generating one molecule of H_2O_2 (*left panel*), which is subsequently caught by vicinal GPx7 to oxidize the *a* domain of PDI (*right panel*). Oxidized PDI can then transfer disulfide bonds to substrates. In this way, a single O_2 molecule generates two disulfide bonds and two H_2O molecules. The detailed mechanism for peroxidase activity of GPx7 is shown in **(B)**: H_2O_2 oxidizes Cys57 of GPx7 to a sulfenic acid, releasing one molecule of water. The sulfenylated Cys57 is then attacked by Cys86 (*left panel*) or the N-terminal cysteine in the CGHC active site of PDI (*right panel*) to form an intra- or inter-molecular disulfide, releasing the second molecule of water. Through further thiol-disulfide exchange, PDI is oxidized and GPx7 is reduced. Only one active domain of PDI is shown here for simplicity. To see this illustration in color, the reader is referred to the web version of this article at www.liebertpub.com/ars

pathways for productive utilization of H_2O_2 in mammalian ER. GPx8, also localizing in close proximity to Ero1α in cells, shows weaker PDI-peroxidase activity *in vitro* (22) and has one order of magnitude lower reactivity with H_2O_2, compared with GPx7 (Fig. 2). Interestingly, GPx8 can prevent accumulation of Ero1α-derived H_2O_2 and ER stress in living cells (Ramming and Appenzeller-Herzog, personal communication), but whether GPx8 could promote oxidative folding by using Ero1α-derived H_2O_2 *in situ* is still an open question. The two-cysteine Prx4 was reported to catalyze disulfide formation *in vitro* and *in vivo* (28, 39). However, Prx4 can be inactivated by H_2O_2, and no enzymes that are capable of reducing over-oxidized Prxs (such as sulfiredoxin) have been found so far in the ER (36). Different from Prx4, GPx7 is hardly inactivated at a sub-millimolar concentration of H_2O_2 (unpublished data), implying that GPx7 is either resistant to over-oxidation or protected by PDI. A certain degree of redundancy of peroxidase activities in the early secretory compartment may be important to optimize oxidative folding while limiting the risks of oxidative stress.

Different from canonical cysteine-based TGPx in invertebrates and plants, GPx7 lacks the corresponding C_R known to confer preferential reducibility by thioredoxin (7). Here, we demonstrate the function of Cys86 to resolve the Cys57 sulfenic acid to form an intramolecular disulfide for PDI oxidation (Fig. 8B, *left panel*). Moreover, the presence of Cys86 also prevents the formation of the less-active GPx7 homodimers bridged by two C_P (Fig. 4C). Therefore, Cys86 emerges as a novel noncanonical C_R. This cysteine residue is conserved in a similar position among almost all GPx members; however, whether the analogues of Cys86 in other TGPx without canonical C_R (*e.g.*, human GPx5) can also play resolving roles is currently unclear. Since the sulfur atoms of the two cysteine residues in reduced GPx7 are located ~11 Å away protein data bank code (PDB: 2P31), it is expected that the formation of the intramolecular disulfide should result in significant conformational changes. The observation that GPx7 C86A can also oxidize PDI, suggests an alternative pathway (Fig. 8B, *right panel*), in which the sulfenylated C_P directly oxidizes PDI *via* an intermolecular disulfide. This is similar to the way in which yeast TGPx Orp1 oxidizes the transcription factor Yap1 (9). Therefore, PDI can react with Cys57 of GPx7, either in the sulfenylated form or in the disulfide form. On the other hand, Cys86 was recently reported to be critical for the formation of GPx7-GRP78 covalent complexes *in vitro*, at an extremely high concentration of H_2O_2 (37). In this case, the possibility that Cys57 was inactivated to -SO_2/SO_3 forms by H_2O_2 cannot be ruled out. Therefore, whether GPx7 could adopt additional ways to interact with its partner proteins still needs further investigation. An interesting feature of GPx7 is that it passes the oxidizing equivalents to PDI rather than directly to GSH (22), and the rate constant for the reduction of GPx7 by PDI is 270-fold faster than that by GSH (6). In this regard, we did not observe any change of oxidized to total glutathione ratio in GPx7-transfected HeLa cells at a steady state (Supplementary Fig. S6). Similarly, Ero1 and Prx4 proteins prefer PDI compared with GSH as substrates (8). In addition, the ER thiol-disulfide homoeostasis is not changed on ectopic expression of WT Ero1α, unless the deregulated hyperactive Ero1α was introduced (1). These results imply that the ER redox homeostasis is tightly controlled, and PDI plays a pivotal role in oxidative folding, preventing futile consumption of GSH and ensuring correct disulfide formation. Moreover, since the chaperone activity and the overall structure of human PDI are redox regulated (32, 33), the oxidation of PDI by GPx7 could result in conformational changes and elevated chaperone activities in cells, which could be another oxidative stress-induced cellular protective pathway.

The observations that GPx7 is down-regulated in breast cancer cells (30) and esophageal adenocarcinoma (23) suggest a tumor suppressor function of GPx7, possibly by preventing cells from high levels of reactive oxygen species and oxidative DNA damage. In accordance with this, *GPx7* knockout mice suffered from systemic oxidative stress damage, increased carcinogenesis, and shortened life span (37). Recently, it was revealed that Ero1α is highly expressed in esophageal and gastric cancer cells (4), further emphasizing the importance of ER redox regulation in the pathophysiology of the gastrointestinal tract. Considering our observations that GPx7 can directly react with Ero1α-derived H_2O_2, it will be very interesting to investigate whether there exists any coincidence and/or correlation between the decrease of GPx7 and increase of Ero1α in the development of these cancers. In view of the key roles of H_2O_2 in cell signaling and pathophysiology, further work is also needed to characterize the network of peroxide in terms of sources (38), scavengers (16), and regulation in the secretory compartment. Emerging evidence on the relationship between disulfide formation and diseases associated with redox imbalance also highlight the enzyme molecules involved in ER redox homeostasis as potential targets for both biomarker and drug development in these diseases.

Materials and Methods

Plasmids and protein purification

The pKEHS780 plasmid encoding the mature human GPx7 (Q20-L187) without signal sequence was a kind gift from L. Ruddock. BL21 (DE3) cells (Novagen) expressing GPx7 were grown in Luria-Bertani medium containing 100 μg/ml of ampicillin at 37°C for 4 h, and shaken for 20 h at 25°C after addition of 200 μ*M* isopropyl-β-D-thiogalactoside. Homogenates from cell lysates were applied onto a Ni-Chelating Sepharose Fast Flow column (GE Healthcare). Fractions eluted with 250 m*M* imidazole were further loaded on a HiPrep 26/10 desalting column (GE Healthcare) that was pre-equilibrated with 50 m*M* Tris-HCl, pH7.6, 150 m*M* NaCl, and 1 m*M* EDTA. The flow-through was concentrated, and aliquots were stored at −80°C. Recombinant mature full-length human Ero1α and PDI proteins were purified as previously described (34).

The cDNA encoding the signal sequence of GPx7 or PDI was added by overlapping PCR using pKEHS780 or pQE30-PDI (34) as a template, and then inserted into pcDNA3.1 vector at *XbaI* and *KpnI* sites to generate plasmids suitable for expression in eukaryotic cells. Mutagenesis was carried out using the Fast Mutagenesis Kit (TransGen) according to the manufacturer's instructions. The pcDNA3.1-Ero1α construct was used as previously described (21), and pcDNA3.1-Ero1α with a C-terminal HA tag was constructed by PCR. Each construct was verified by DNA sequencing.

Cell culture, transfection, and antibodies

HeLa cells were maintained in Dulbecco's modified Eagle's medium (DMEM; Gibco) supplemented with 5% fetal bovine

serum (Gibco), 100 units/ml penicillin, and 100 μg/ml streptomycin (Gibco) at 5% CO_2. HeLa cells were transfected using Lipofectamine2000 (Invitrogen) according to the manufacturer's instructions.

Antibodies to GPx7 were obtained from rabbits on immunization with purified GPx7 protein as an adjuvant. Mouse monoclonal anti-Ero1α (2G4) and anti-myc (9E10) were used as described (24), while anti-PDI (RL90) and anti-GAPDH (6C5) were purchased from Abcam and Beyotime, respectively.

RNA interference

For transient knockdown of Ero1α, pSUPER-retro-puro retrovirus vector (Oligoengine) expressing shRNA targeting Ero1α sequence 5′-GGGACACAACATTACAGAATTTCAA-3′ (10) was constructed following the manufacturer's instructions. The resulting shEro1α plasmid was transfected into HeLa cells combined with JcM plasmid on day 1, followed by a second-round transfection of shEro1α plasmid with GPx7 plasmid on day 3 and subsequent analysis on day 5.

Enzyme activity assays

Denatured and reduced RNase A was prepared as described (19). For oxygen consumption assays, all components except Ero1α were mixed and added to an Oxygraph Clark-type electrode (Hansatech Instruments), followed by an injection of Ero1α to initiate the reaction. For H_2O_2 determination, catalase at 20 μg/ml was injected into the reaction vessel when the thiol oxidation reaction was complete.

RNase A reactivation was assayed by monitoring the 296 nm absorbance increase at 25°C due to the hydrolysis of cCMP as described (34).

GPx activity was measured using a coupled assay after the decrease in absorbance at 340 nm due to reduced nicotinamide adenine dinucleotide phosphate (NADPH) (0.15 m*M*; Roche) consumption by glutathione reductase (0.24 unit; Sigma) (22), with addition of H_2O_2 or Ero1α to start the reaction. A molar extinction coefficient of 6200 $M^{-1} \cdot cm^{-1}$ for NADPH was used for calculations. All experiments were performed in 100 m*M* Tris-HAc (pH 8.0) containing 50 m*M* NaCl and 1 m*M* EDTA.

Stopped-flow fluorescence

The oxidation rate of the active site of GPx7 was determined by the decrease of tryptophan fluorescence using a PiStar-180 stopped-flow fluorometer (Applied Photophysics) with an excitation at 280 nm and a band–pass emission >320 nm at 25°C. The reaction was started by an injection of 0–10 m*M* H_2O_2 into 10 μ*M* GPx7 in 100 m*M* citrate (pH 7.0), 200 m*M* Na_2HPO_4, and 1 m*M* EDTA.

In vivo *oxidative folding assays*

HeLa transfectants expressing JcM were incubated for 5 min at 37°C with 5 m*M* DTT in DMEM, washed twice with ice-cold phosphate-buffered saline (PBS), and cultured in DMEM without DTT at an indicated temperature (5). Aliquots were taken at different times, quenched with 20 m*M* N-ethylmaleimide (NEM), lysed in radio immunoprecipitation assay buffer (Beyotime) with NEM and protease inhibitors, and resolved by nonreducing sodium dodecyl sulfate-polyacrylamide gel electrophoresis (SDS-PAGE). Western blots (WB) were developed by anti-myc and enhanced chemiluminescence (ECL) (Thermo Scientific), followed by using a ChemiScope mini chemiluminescence imaging system (Clinx Science). Band intensities were quantified by densitometry using ImageJ software.

In vitro *redox-state measurements, mixed disulfides trapping, and sulfenic acid detection*

To measure the redox states of GPx7, 20 μ*M* recombinant GPx7 proteins were incubated with or without 40 μ*M* H_2O_2 for 15 min. Free thiols were then blocked by adding 2 m*M* AMS (Invitrogen). For PDI oxidation assays, reactions were initiated by adding 20 μ*M* H_2O_2 to 20 μ*M* GPx7 and 20 μ*M* reduced PDI *a* domain, and samples were taken for quenching using 2 m*M* AMS at the indicated times. To trap the disulfide-linked complex between GPx7 and PDI, 20 μ*M* GPx7 and 10 μ*M* PDI C56A proteins were mixed for 15 min and then blocked by 20 m*M* NEM. Samples were then analyzed by SDS-PAGE and Coomassie staining. For sulfenic acid detection, 50 μ*M* GPx7 proteins were incubated with 100 μ*M* H_2O_2 and 1 m*M* DCP-Bio1 (KeraFAST) for 30 min. Excess DCP-Bio1 was removed by using Amicon Ultra centrifugal filters (Millipore). Samples were then analyzed by SDS-PAGE, developed by either Coomassie staining or WB using horseradish peroxidise-labeled streptavidin (Beyotime) and ECL. All experiments were performed at 25°C in PBS buffer.

Pulldown assays and trapping mixed disulfides in vivo

For pulldown assay, Glutathione Sepharose resins (GE Healthcare) were incubated with 10 μ*M* GST-GPx7 fusion proteins and HeLa lysates (0.5 mg protein/ml) for 4 h at 4°C in PBS, and washed five times with ice-cold PBS. Bound proteins were detected by Ponceau staining and WB, respectively.

To trap mixed disulfides *in vivo*, HeLa transfectants were incubated for 10 min at 37°C with or without 5 m*M* DTT in DMEM, quenched with 40 m*M* NEM immediately or after DTT washout followed by incubation in DTT-free medium for 30 min. Samples were lysed and analyzed by nonreducing or reducing SDS-PAGE and WB.

Acknowledgments

The authors thank Lloyd Ruddock for the kind gift of pKEHS780 plasmid, Jiangyun Wang for generously providing a cell culture room, Si Wu for technical assistance in stopped-flow determination, and Xi Wang, Xi'e Wang, and Claudio Fagioli for invaluable help. This work was supported by grants from the Chinese Ministry of Science and Technology (2011CB910303 and 2012CB911002) to C.C.W., the National Natural Science Foundation of China (31000351 and 31370775) to L.W., and Telethon (GGP11077) and Associazione Italiana Ricerca Cancro (AIRC; IG and 5×1000 program) to R.S.

Author Disclosure Statement

The authors declare that they have no conflicts of interest.

References

1. Appenzeller-Herzog C, Riemer J, Christensen B, Sorensen ES, and Ellgaard L. A novel disulphide switch mechanism in Ero1 alpha balances ER oxidation in human cells. *EMBO J* 27: 2977–2987, 2008.
2. Araki K and Inaba K. Structure, mechanism, and evolution of Ero1 family enzymes. *Antioxid Redox Signal* 16: 790–799, 2012.

3. Baker KM, Chakravarthi S, Langton KP, Sheppard AM, Lu H, and Bulleid NJ. Low reduction potential of Ero1 alpha regulatory disulphides ensures tight control of substrate oxidation. *EMBO J* 27: 2988–2997, 2008.
4. Battle D, Gunasekara SD, Watson G, Ahmed EM, Saysell C, Altaf N, Sanusi A, Munipalle P, Scoones D, Walker J, Viswanath Y, and Benham A. Expression of the endoplasmic reticulum oxidoreductase Ero1α in gastro-intestinal cancer reveals a link between homocysteine and oxidative protein folding. *Antioxid Redox Signal* 19: 24–35, 2013.
5. Bertoli G, Simmen T, Anelli T, Molteni SN, Fesce R, and Sitia R. Two conserved cysteine triads in human Ero1alpha cooperate for efficient disulfide bondformation in the endoplasmic reticulum. *J Biol Chem* 279: 30047–30052, 2004.
6. Bosello-Travain V, Conrad M, Cozza G, Negro A, Quartesan S, Rossetto M, Roveri A, Toppo S, Ursini F, Zaccarin M, and Maiorino M. Protein disulfide isomerase and glutathione are alternative substrates in the one Cys catalytic cycle of glutathione peroxidase 7. *Biochim Biophys Acta* 1830: 3846–3857, 2013.
7. Brigelius-Flohé R and Maiorino M. Glutathione peroxidases. *Biochim Biophys Acta* 1830: 3289–3303, 2013.
8. Bulleid NJ and Ellgaard L. Multiple ways to make disulfides. *Trends Biochem Sci* 36: 485–492, 2011.
9. Delaunay A, Pflieger D, Barrault MB, Vinh J, and Toledano MB. A thiol peroxidase is an H_2O_2 receptor and redox-transducer in gene activation. *Cell* 111: 471–481, 2002.
10. Enyedi B, Varnai P, and Geiszt M. Redox state of the endoplasmic reticulum is controlled by Ero1L-alpha and ntraluminal calcium. *Antioxid Redox Signal* 13: 721–729, 2010.
11. Gross E, Sevier CS, Heldman N, Vitu E, Bentzur M, Kaiser CA, Thorpe C, and Fass D. Generating disulfides enzymatically: reaction products and electron acceptors of the endoplasmic reticulum thiol oxidase Ero1p. *Proc Natl Acad Sci U S A* 103: 299–304, 2006.
12. Hatahet F and Ruddock LW. Protein disulfide isomerase: a critical evaluation of its function in disulfide bond formation. *Antioxid Redox Signal* 11: 2807–2850, 2009.
13. Inaba K, Masui S, Iida H, Vavassori S, Sitia R, and Suzuki M. Crystal structures of human Ero1α reveal the mechanisms of regulated and targeted oxidation of PDI. *EMBO J* 29: 3330–3343, 2010.
14. Iuchi Y, Okada F, Tsunoda S, Kibe N, Shirasawa N, Ikawa M, Okabe M, Ikeda Y, and Fujii J. Peroxiredoxin 4 knockout results in elevated spermatogenic cell death via oxidative stress. *Biochem J* 419: 149–158, 2009.
15. Jessop CE, Watkins RH, Simmons JJ, Tasab M, and Bulleid NJ. Protein disulphide isomerase family members show distinct substrate specificity: P5 is targeted to BiP client proteins. *J Cell Sci* 122: 4287–4295, 2009.
16. Kakihana T, Nagata K, and Sitia R. Peroxides and peroxidases in the endoplasmic reticulum: integrating redox homeostasis and oxidative folding. *Antioxid Redox Signal* 16: 763–771, 2012.
17. Karala AR, Lappi AK, Saaranen MJ, and Ruddock LW. Efficient peroxide-mediated oxidative refolding of a protein at physiological pH and implications for oxidative folding in the endoplasmic reticulum. *Antioxid Redox Signal* 11: 963–970, 2009.
18. Klomsiri C, Nelson KJ, Bechtold E, Soito L, Johnson LC, Lowther WT, Ryu SE, King SB, Furdui CM, and Poole LB. Use of dimedone-based chemical probes for sulfenic acid detection: evaluation of conditions affecting probe incorporation into redox-sensitive proteins. *Method Enzymol* 473: 77–94, 2010.
19. Lyles MM and Gilbert HF. Catalysis of the oxidative folding of ribonuclease A by protein disulfide isomerase: dependence of the rate on the composition of the redox buffer. *Biochemistry* 30: 613–619, 1991.
20. Margittai E, Loew P, Stiller I, Greco A, Garcia-Manteiga JM, Pengo N, Benedetti A, Sitia R, and Banhegyi G. Production of H_2O_2 in the endoplasmic reticulum promotes *in vivo* disulfide bond formation. *Antioxid Redox Signal* 16: 1088–1099, 2012.
21. Mezghrani A, Fassio A, Benham A, Simmen T, Braakman I, and Sitia R. Manipulation of oxidative protein folding and PDI redox state in mammalian cells. *EMBO J* 20: 6288–6296, 2001.
22. Nguyen VD, Saaranen MJ, Karala AR, Lappi AK, Wang L, Raykhel IB, Alanen HI, Salo KEH, Wang CC, and Ruddock LW. Two endoplasmic reticulum PDI peroxidases increase the efficiency of the use of peroxide during disulfide bond formation. *J Mol Biol* 406: 503–515, 2011.
23. Peng DF, Belkhiri A, Hu TL, Chaturvedi R, Asim M, Wilson KT, Zaika A, and El-Rifai W. Glutathione peroxidase 7 protects against oxidative DNA damage in oesophageal cells. *Gut* 61: 1250–1260, 2012.
24. Ronzoni R, Anelli T, Brunati M, Cortini M, Fagioli C, and Sitia R. Pathogenesis of ER storage disorders: modulating russell body biogenesis by altering proximal and distal quality control. *Traffic* 11: 947–957, 2010.
25. Schulman S, Wang B, Li WK, and Rapoport TA. Vitamin K epoxide reductase prefers ER membrane-anchored thioredoxin-like redox partners. *Proc Natl Acad Sci U S A* 107: 15027–15032, 2010.
26. Sevier CS and Kaiser CA. Ero1 and redox homeostasis in the endoplasmic reticulum. *Biochim Biophys Acta* 1783: 549–556, 2008.
27. Sevier CS, Qu HJ, Heldman N, Gross E, Fass D, and Kaiser CA. Modulation of cellular disulfide-bond formation and the ER redox environment by feedback-regulation of Ero1. *Cell* 129: 333–344, 2007.
28. Tavender TJ, Springate JJ, and Bulleid NJ. Recycling of peroxiredoxin IV provides a novel pathway for disulphide formation in the endoplasmic reticulum. *EMBO J* 29: 4185–4197, 2010.
29. Toppo S, Vanin S, Bosello V, and Tosatto SCE. Evolutionary and structural insights into the multifaceted glutathione peroxidase (Gpx) superfamily. *Antioxid Redox Signal* 10: 1501–1513, 2008.
30. Utomo A, Jiang XZ, Furuta S, Yun J, Levin DS, Wang YCJ, Desai KV, Green JE, Chen PL, and Lee WH. Identification of a novel putative non-selenocysteine containing phospholipid hydroperoxide glutathione peroxidase (NPGPx) essential for alleviating oxidative stress generated from polyunsaturated fatty acids in breast cancer cells. *J Biol Chem* 279: 43522–43529, 2004.
31. van Lith M, Tiwari S, Pediani J, Milligan G, and Bulleid NJ. Real-time monitoring of redox changes in the mammalian endoplasmic reticulum. *J Cell Sci* 124: 2349–2356, 2011.
32. Wang C, Li W, Ren J, Fang J, Ke H, Gong W, Feng W, and Wang CC. Structural insights into the redox-regulated dynamic conformations of human protein disulfide isomerase. *Antioxid Redox Signal* 19: 36–45, 2013.
33. Wang C, Yu J, Huo L, Wang L, Feng W, and Wang CC. Human protein-disulfide isomerase is a redox-regulated chaperone activated by oxidation of domain a'. *J Biol Chem* 287: 1139–1149, 2012.
34. Wang L, Li SJ, Sidhu A, Zhu L, Liang Y, Freedman RB, and Wang CC. Reconstitution of human Ero1-Lalpha/protein-disulfide isomerase oxidative folding pathway *in vitro*. Position-dependent differences in role between the a and a' domains of protein-disulfide isomerase. *J Biol Chem* 284: 199–206, 2009.
35. Wang L, Zhu L, and Wang CC. The endoplasmic reticulum sulfhydryl oxidase Ero1 beta drives efficient oxidative protein folding with loose regulation. *Biochem J* 434: 113–121, 2011.

36. Wang X, Wang L, Wang Xe, Sun F, and Wang CC. Structural insights into the peroxidase activity and inactivation of human peroxiredoxin 4. *Biochem J* 441: 113–118, 2012.
37. Wei P-C, Hsieh Y-H, Su M-I, Jiang X, Hsu P-H, Lo W-T, Weng J-Y, Jeng Y-M, Wang J-M, Chen P-l, Chang Y-C, Lee K-F, Tsai M-D, Shew J-Y, and Lee W-H. Loss of the oxidative stress sensor NPGPx compromises GRP78 chaperone activity and induces systemic disease. *Mol Cell* 48: 747–759, 2012.
38. Zito E, Hansen HG, Yeo GSH, Fujii J, and Ron D. Endoplasmic reticulum thiol oxidase deficiency leads to ascorbic acid depletion and noncanonical scurvy in mice. *Mol Cell* 48: 39–51, 2012.
39. Zito E, Melo EP, Yang Y, Wahlander A, Neubert TA, and Ron D. Oxidative protein folding by an endoplasmic reticulum-localized peroxiredoxin. *Mol Cell* 40: 787–797, 2010.

Address correspondence to:
Dr. Lei Wang
National Laboratory of Biomacromolecules
Institute of Biophysics
Chinese Academy of Sciences
Beijing 100101
China

E-mail: wanglei@moon.ibp.ac.cn

Prof. Chih-chen Wang
National Laboratory of Biomacromolecules
Institute of Biophysics
Chinese Academy of Sciences
Beijing 100101
China

E-mail: chiwang@sun5.ibp.ac.cn

Date of first submission to ARS Central, February 8, 2013; date of final revised submission, July 18, 2013; date of acceptance, August 6, 2013.

Abbreviations Used

AMS = 4-acetamido-4′-maleimidylstilbene-2,2′-disulfonic acid
C_P = peroxidatic cysteine
C_R = resolving cysteine
DCP-Bio1 = 3-(2,4-dioxocyclohexyl) propyl with a biotin tag
DMEM = Dulbecco's modified Eagle's medium
DTT = dithiothreitol
ECL = enhanced chemiluminescence
ER = endoplasmic reticulum
GPx7 = glutathione peroxidase 7
GSH = reduced glutathione
GSSG = oxidized glutathione
GST = glutathione S-transferase
JcM = myc-tagged Ig-J chains
NADPH = reduced nicotinamide adenine dinucleotide phosphate
NEM = N-ethylmaleimide
PBS = phosphate-buffered saline
PDI = protein disulfide isomerase
Prx4 = peroxiredoxin 4
SDS-PAGE = sodium dodecyl sulfate-polyacrylamide gel electrophoresis
WB = Western blots
WT = wild-type